



Research
Bridge Engineering—Article

Wind-Tunnel Investigation of the Aerodynamic Performance of Surface-Modification Cables

Hiroshi Katsuchi^{a,*}, Hitoshi Yamada^a, Ippei Sakaki^b, Eiichi Okado^b

^aYokohama National University, Yokohama 240-8501, Japan

^bShinko Wire Company, Ltd., Amagasaki 660-0091, Japan

ARTICLE INFO

Article history:

Received 11 May 2017

Revised 25 June 2017

Accepted 28 June 2017

Available online 29 September 2017

Keywords:

Rain-wind-induced vibration

Dry galloping

Stay cable

Wind-tunnel test

ABSTRACT

The wind-induced vibration of stay cables of cable-stayed bridges, which includes rain-wind-induced vibration (RWIV) and dry galloping (DG), has been studied for a considerable amount of time. In general, mechanical dampers or surface modification are applied to suppress the vibration. In particular, several types of surface-modification cable, including indentation, longitudinally parallel protuberance, helical fillet, and U-shaped grooving, have been developed. Recently, a new type of aerodynamically stable cable with spiral protuberances was developed. It was confirmed that the cable has a low drag force coefficient, like an indented cable, and that it prevented the formation of water rivulets on the cable surface. In this study, the stability for RWIV of this cable was investigated with various flow angles and protuberance dimensions in a wind-tunnel test. It was found that the spiral protuberance cable is aerodynamically stable against both RWIV and DG for all test wind angles. The effects of the protuberance dimensions were also clarified.

© 2017 THE AUTHORS. Published by Elsevier LTD on behalf of Chinese Academy of Engineering and Higher Education Press Limited Company. This is an open access article under the CC BY-NC-ND license (<http://creativecommons.org/licenses/by-nc-nd/4.0/>).

1. Introduction

The stay cables of cable-stayed bridges are subject to aerodynamic excitation forces due to their oblique attitude against the wind. They sometimes exhibit large-amplitude vibration, not only under rain conditions but also under dry (no rain) conditions. The former is referred to as rain-wind-induced vibration (RWIV) [1] and the latter is referred to as dry galloping (DG); there are many studies [2,3] on their mechanisms. It is understood that both vibrations are related to the inherent instability of inclined cables; in particular, RWIV is caused by water rivulets running down the cable surface and DG is caused by the suppression of Karman vortices in the critical Reynolds number range together with an axial flow behind the cable. Considering their vibration mechanisms, some surface-modification cables were developed that included spiral protuberances [4], longitudinally parallel protuberances [5], and indentations [6]. In order to further improve cable performance, a new type of surface-modification cable with prefabricated spiral protuberances was recently developed [7]. For a surface modification, attention must be paid to the increase in the drag force coefficient (C_D). The newly developed spiral

protuberance cable was tested for C_D in an independent study and it was confirmed that the C_D of the new cable was as low as that of the indented cable [7]. In this study, using a renovated wind tunnel with a rain simulator system, the performance of two surface-modification cables, including the spiral protuberance and the indented cables, was investigated.

2. Experimental facility

The RWIV was reproduced in the wind-tunnel facility with a rain simulator at the Yokohama National University. An old wind tunnel was renovated by replacing a working section and equipping water spray nozzles, as shown in Fig. 1. The working section with the rain simulator was placed just at the wind-tunnel exit, which was 1.3 m in width and 1.3 m in height. Water was sprayed from water spray nozzles on the ceiling of the working section, as shown in Fig. 2. The maximum wind speed was about $20 \text{ m}\cdot\text{s}^{-1}$.

A cable model of 1.5 m in effective length was placed in the working section using a pipe frame, as shown in Fig. 3. The model was supported by coil springs with one vertical degree of freedom. The coil springs were attached in the direction normal to the cable axis. The flow yaw angle and the vertical angle could be adjusted by rotating and lifting/lowering one side of the pipe frame, respectively. There are some discussions on the “end effect” of a cable

* Corresponding author.

E-mail address: katsuchi@ynu.ac.jp (H. Katsuchi).

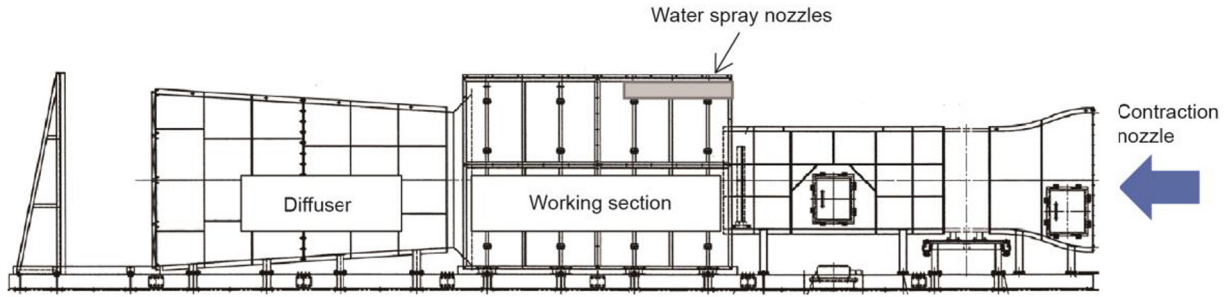


Fig. 1. Rain-wind simulator.



Fig. 2. Working section and rain simulator.

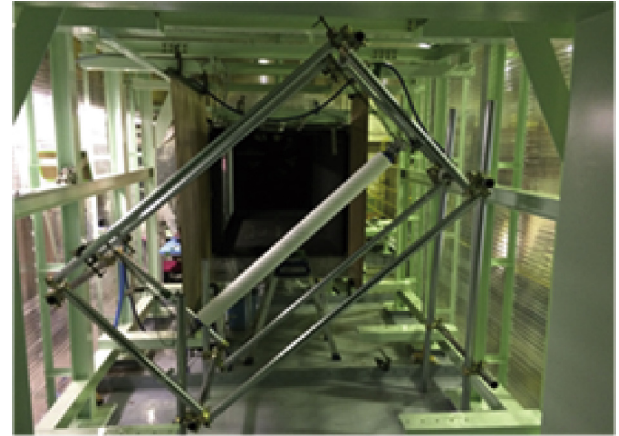


Fig. 3. Cable model setup.

model. In this study, a whole cable model without end-effect treatment was exposed to a wind flow. This was done to avoid unknown effects due to the end-effect treatment, as the main objective of this study was a comparison among different cases.

The response of the model was measured by accelerometers placed on both ends of the model. Model vibration was measured with a sampling frequency of 100 Hz. The natural frequency of the model was 0.8–1.0 Hz, depending on the test cases.

3. Reproduction of RWIV

In order to check the performance of the wind tunnel and rain simulator, a circular cable model of a 1.5 m long polyethylene pipe

was tested to reproduce RWIV. Two different diameter models of 110 mm (D110 mm) and 158 mm (D158 mm) were tested. Figs. 4 and 5 show the response amplitude versus the wind speed for the D110 mm and D158 mm cases, respectively. The Scruton number (S_c) was set to small, from 3 to 11, in order to generate RWIV easily, as described in the figure caption. In this study, S_c is defined as follows:

$$S_c = \frac{2m\delta}{\rho D^2} \quad (1)$$

where m is the mass per unit length, δ is the structural damping of the logarithmic decrement, ρ is the air density, and D is the model diameter. Due to the model support mechanism, damping in small vertical angle cases tends to be small; therefore, S_c in those cases is relatively small. The vertical angle (α) was changed to 40° and 25° for the D110 mm case, and to 40°, 25°, and 9° for the D158 mm case. The flow yaw angle (β) was changed to 0°, 15°, 30°, 45°, and 60°.

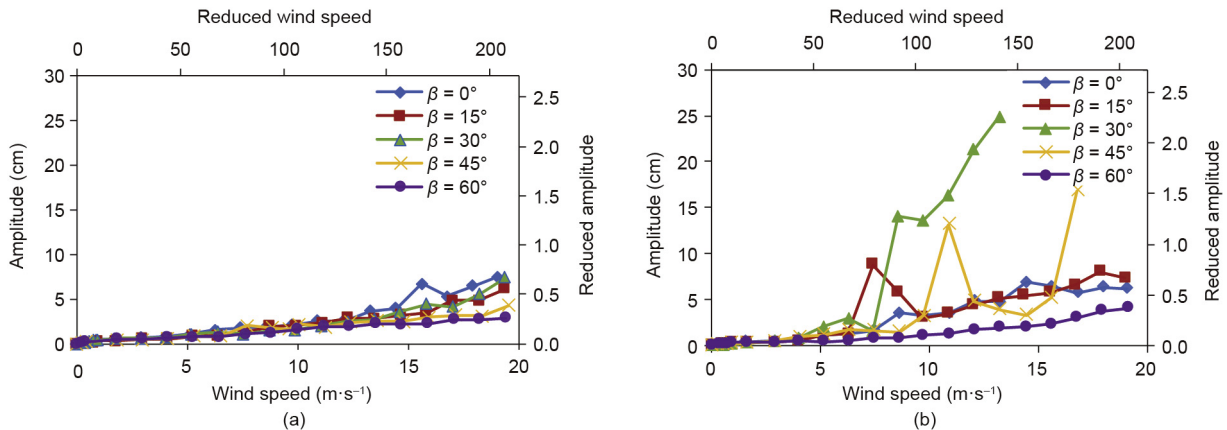


Fig. 4. Response amplitude of circular cable model vs. wind speed under rain conditions (D110 mm). (a) $\alpha = 40^\circ$ ($S_c = 10\text{--}11$); (b) $\alpha = 25^\circ$ ($S_c = 9\text{--}11$).

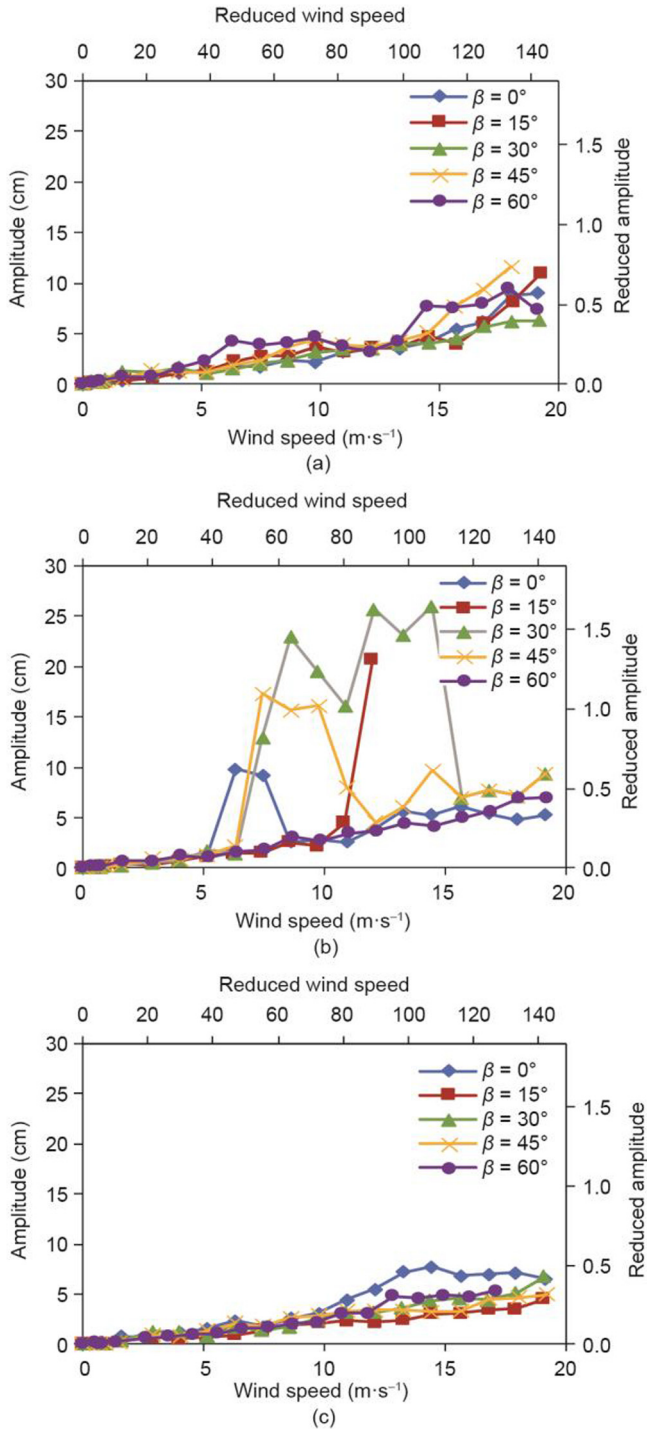


Fig. 5. Response amplitude of circular cable model vs. wind speed under rain conditions (D158 mm). (a) $\alpha = 40^\circ$ ($S_c = 7\text{--}9$); (b) $\alpha = 25^\circ$ ($S_c = 6\text{--}9$); (c) $\alpha = 9^\circ$ ($S_c = 3\text{--}4$).

Large-amplitude RWIV took place only at $\alpha = 25^\circ$ with $\beta = 15^\circ, 30^\circ,$ and 45° , as shown in Figs. 4 and 5. It did not take place at $\alpha = 40^\circ$ and 9° . Measurement was stopped when the vibration amplitude reached around 25 cm in order to prevent supporting system failure. This large-amplitude vibration was observed in the case of $\alpha = 25^\circ$ with $\beta = 30^\circ$. On the other hand, vibration increased considerably at the wind speed of $16 \text{ m}\cdot\text{s}^{-1}$, even more after the first peak at $11 \text{ m}\cdot\text{s}^{-1}$ in the case of D110 mm, and $\alpha = 25^\circ$ with $\beta = 45^\circ$. The first peak was RWIV, while the second large vibration was caused by the mechanism of DG, since no water rivulet formed on the cable surface.

During RWIV, a thin-film-like water rivulet formed on the cable surface. The rivulet vibrated in the circumferential direction synchronously with the cable vibration. The characteristics of the RWIV and rivulet are quite similar to those observed in past studies [8]. The rain intensity during RWIV was $40\text{--}60 \text{ mm}\cdot\text{h}^{-1}$, which was heavy. The rain intensity was adjusted such that RWIV took place in this study. Although the effect of the rain intensity must also depend on cable length, a detailed discussion is not made here.

4. Response of surface-modification cables under rain conditions

As already described, several surface-modification cables were developed for RWIV countermeasures. In this study, two types of surface-modification cable—spiral protuberance [7] and indented [6] cables—were tested for RWIV, as shown in Fig. 6.

The indentation geometry followed the prototype pattern (Fig. 6(c)) that was adopted for the Tataro Bridge, which was the first to use indented cables. Eight indented patterns are placed equally and circumferentially on the surface. The depth of the indentation is 1 mm.

In addition, some parameter tests for the spiral protuberance cables were conducted. The models were supported in the same manner as in the circular model case, as shown in Fig. 7. The S_c con-

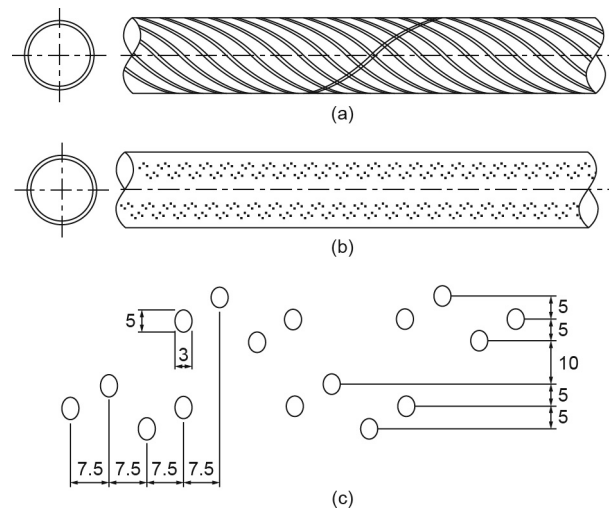


Fig. 6. Surface-modification cables. (a) Spiral protuberance cable; (b) indented cable; (c) dimensions of indentation (unit: mm).

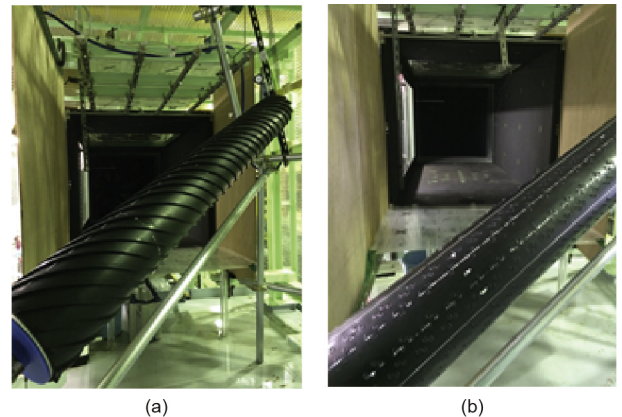


Fig. 7. Setup of surface-modification cable models. (a) Spiral protuberance cable; (b) indented cable.

dition was also nearly the same as that of the circular model case, which is shown in the figure for each case.

4.1. Response characteristics of spiral protuberance and indented cables

Figs. 8 and 9 show the response amplitude of the spiral protuberance and of the indented cables with the diameter of 158 mm, respectively, under rain conditions. RWIV took place in the case of the indented cable at some angles. It was observed that

some water rivulets passed over the indentations during RWIV. However, it is understood that the RWIV observed in this study was due to S_c being much smaller than in a full-scale condition. On the other hand, the spiral protuberance cable did not exhibit RWIV for all cases, but only for cases with small-amplitude random vibration.

4.2. Effects of spiral protuberance dimensions on response

The dimensions of the spiral protuberance were decided based on a past study [7]. The original dimensions were optimized so as to keep C_o low and to prevent water rivulet formation at the same time. The basic dimensions are: 12 circumferential protuberances

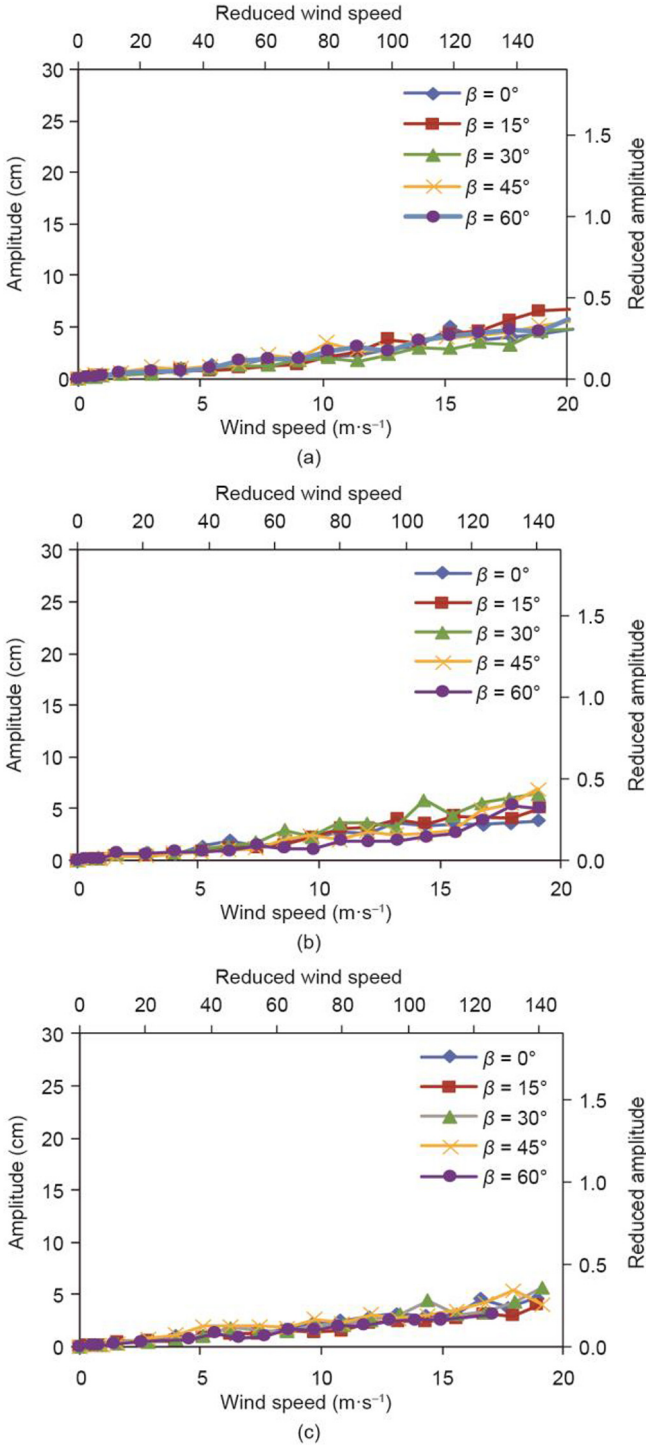


Fig. 8. Response amplitude of spiral protuberance cable model vs. wind speed under rain conditions (D158 mm). (a) $\alpha = 40^\circ$ ($S_c = 9$); (b) $\alpha = 25^\circ$ ($S_c = 5-12$); (c) $\alpha = 9^\circ$ ($S_c = 4$).

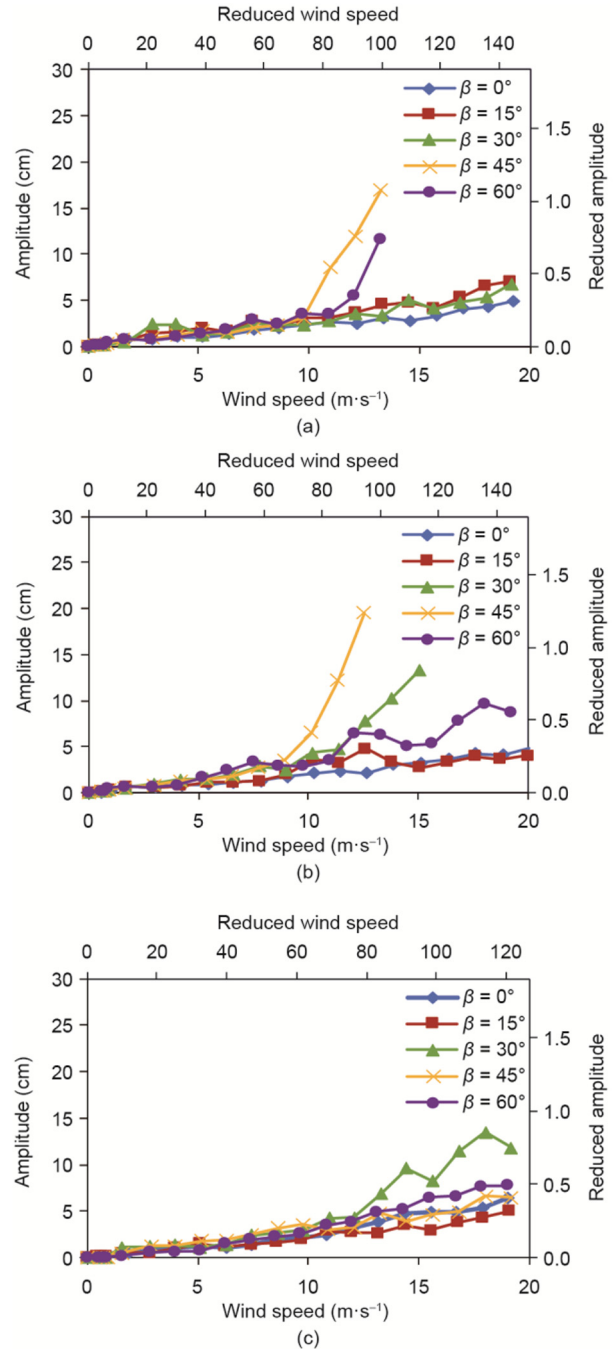


Fig. 9. Response amplitude of indented cable model vs. wind speed under rain condition (D158 mm). (a) $\alpha = 40^\circ$ ($S_c = 8-9$); (b) $\alpha = 25^\circ$ ($S_c = 5-8$); (c) $\alpha = 9^\circ$ ($S_c = 3-4$).

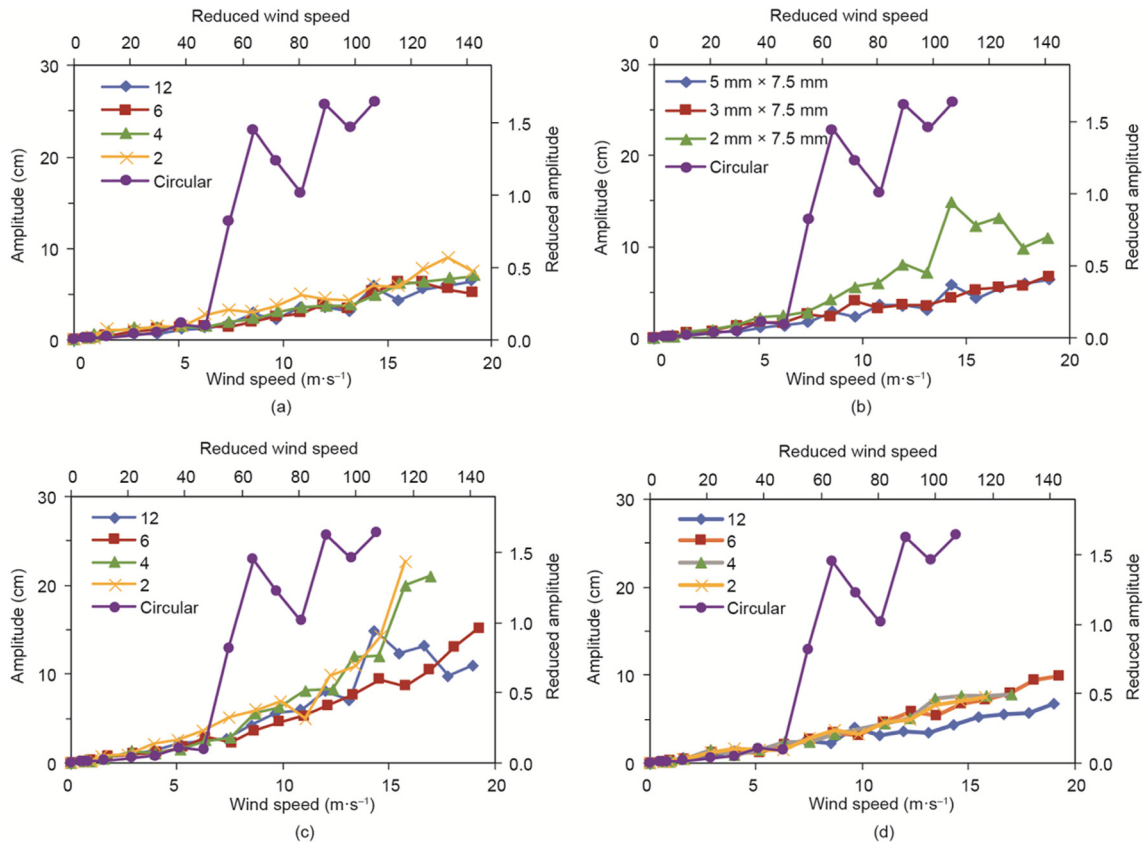


Fig. 10. Response amplitude of spiral protuberances cable model vs. wind speed for different spiral protuberance dimensions under rain condition ($D158$ mm, $\alpha = 25^\circ$, $\beta = 30^\circ$). (a) Number of spiral protuberances (5 mm height); (b) size of spiral protuberance (height \times width) (12 protuberances); (c) number of spiral protuberances (2 mm height); (d) number of spiral protuberances (3 mm height).

of 5 mm in height and 7.5 mm in width, with a spiral angle of 27° . However, the effects of the spiral protuberance dimensions were only confirmed in a wind tunnel under dry (no rain) conditions for DG at that time. Therefore, it is desirable to confirm the effects of the spiral protuberance dimensions under rain conditions for RWIV.

A significant effect of the number of spiral protuberances is not observed as long as the 5 mm height is kept, as shown in Fig. 10(a). However, a slight increase in the amplitude is found in the case of two protuberances. In order to investigate the minimum height of the spiral protuberance, dimensions of 2 mm and 3 mm height were tested, while keeping 12 protuberances and a width of 7.5 mm. It was found that the 2 mm height case increased the vibration amplitude significantly, as shown in Fig. 10(b).

Further investigation on the effects of height and number of spiral protuberances was conducted. The 2 mm height increased the RWIV amplitude more than the basic 5 mm height case, even with 12 protuberances, as shown in Fig. 10(c). For 3 mm height, a decrease in spiral protuberance number affected the vibration amplitude, as shown in Fig. 10(d). The case of 12 protuberances only prevented an increase in the RWIV amplitude. Therefore, if the number of spiral protuberances is kept at the original number of 12, a protuberance height of 5 mm is desirable.

5. DG of surface-modification cables

In addition to RWIV, DG was tested for the surface-modification cable model. Fig. 11 shows the response amplitude of the spiral protuberance cable model under dry (no rain) conditions, compared with the circular cable model case.

The cause of DG was explained mainly in terms of the critical Reynolds number flow regime and the axial flow behind an inclined cable [3]. However, a large-amplitude vibration was also observed under dry (no rain) conditions at the subcritical range for the inclined stay cables of a full-scale bridge [2]. Therefore, this study also deals with divergent large-amplitude vibration under dry (no rain) conditions as DG in a broad sense.

The circular cable model exhibited large-amplitude DG, particularly with the flow angles of $\beta = 30^\circ$ and 45° . However, these vibrations occurred with a low S_c of up to 10, which is relatively lower than that of full-scale cables. It was confirmed that large-amplitude DG was suppressed below the reduced amplitude of 0.5 with an increase in S_c to around 60. On the other hand, the spiral protuberance cable model was completely stable and exhibited only small-amplitude random vibration.

6. Conclusions

In this study, the performance of two kinds of surface-modification cables was investigated using a renovated wind tunnel with a rain simulator system. The following results were obtained.

RWIV was successfully reproduced in the wind tunnel. It was also observed that the water rivulet on the cable surface vibrated in the circumferential direction synchronously with the cable vibration. These characteristics coincide well with past studies.

The indented surface-modification cable showed good performance for both RWIV and DG, except under some particular conditions. However, the increase in S_c can suppress vibrations. The spiral protuberance cable showed thoroughly good performance for both RWIV and DG.

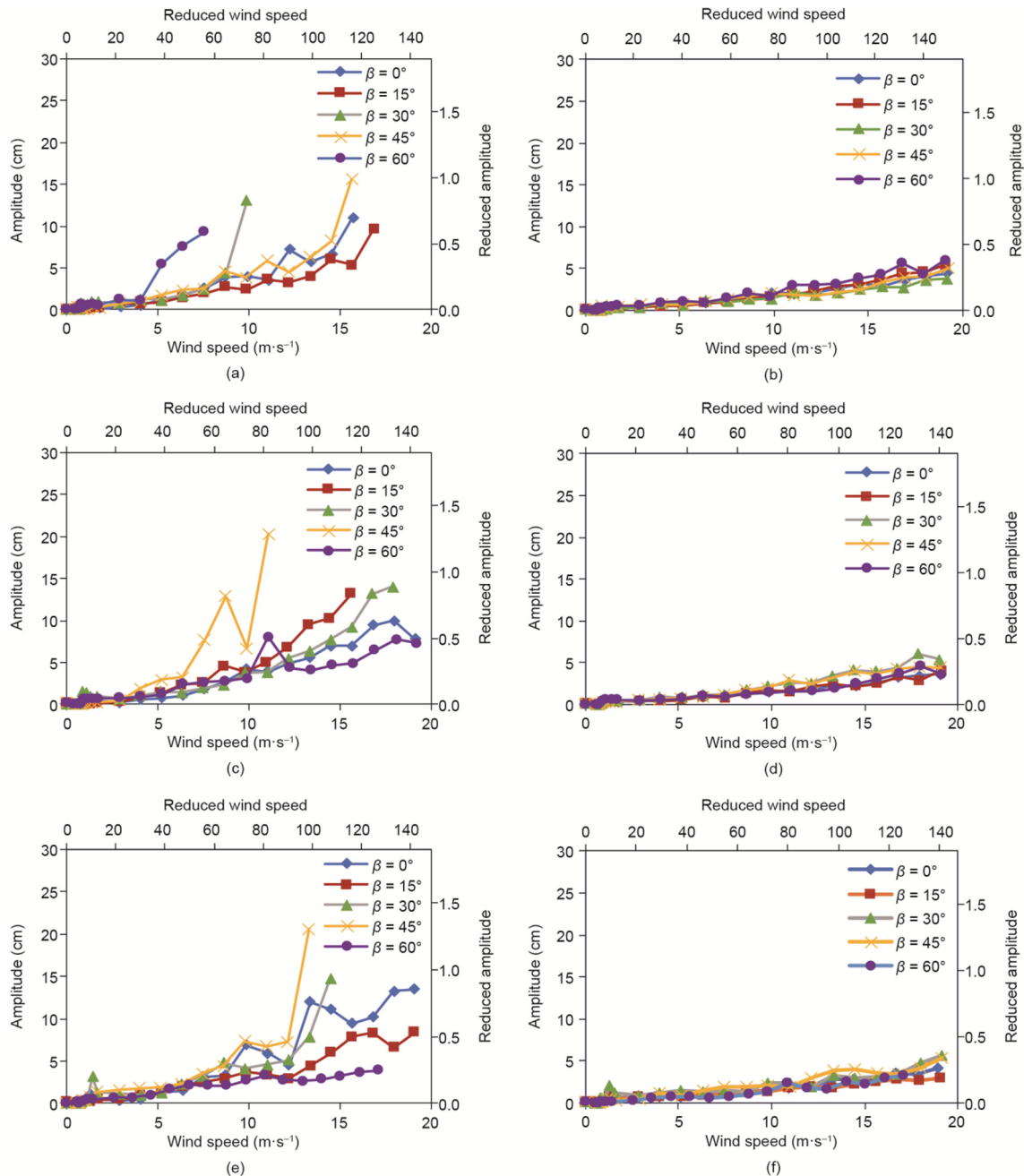


Fig. 11. Response amplitude vs. wind speed under dry (no rain) conditions (D158 mm). (a) Circular, $\alpha = 40^\circ$ ($S_c = 7\text{--}9$); (b) spiral protuberance, $\alpha = 40^\circ$ ($S_c = 9$); (c) circular, $\alpha = 25^\circ$ ($S_c = 6\text{--}9$); (d) spiral protuberance, $\alpha = 25^\circ$ ($S_c = 5\text{--}12$); (e) circular, $\alpha = 9^\circ$ ($S_c = 3\text{--}4$); (f) spiral protuberance, $\alpha = 9^\circ$ ($S_c = 4$).

Finally, the effects of the spiral protuberance dimensions were clarified. Certain limits in the dimensions, such as height and protuberance number, are required in order to suppress RWIV.

Compliance with ethics guidelines

Hiroshi Katsuchi, Hitoshi Yamada, Ippei Sakaki, and Eiichi Okado declare that they have no conflict of interest or financial conflicts to disclose.

References

- [1] Hikami Y, Shiraishi N. Rain-wind induced vibrations of cables stayed bridges. *J Wind Eng Ind Aerod* 1988;29(1-3):409–18.
- [2] Zuo D, Jones NP. Interpretation of field observations of wind- and rain-wind-induced stay cable vibrations. *J Wind Eng Ind Aerod* 2010;98(2):73–87.
- [3] Matsumoto M. On generation mechanism of “rain vibration” and “dry galloping” of inclined stayed cables of cable-stayed bridges, basing on their flow fields. In: *Proceedings of the 9th International Symposium on Cable Dynamics*; 2011 Oct 18–20; Shanghai, China. p. 207–14.
- [4] Flamand O. Rain-wind induced vibration of cables. *J Wind Eng Ind Aerod* 1995;57(2-3):353–62.
- [5] Saito T, Matsumoto M, Kitazawa M. Rain-wind excitation of cables on cable-stayed Higashi-Kobe Bridge and cable vibration control. In: *Proceedings of the International Conference on Cable-Stayed and Suspension Bridges*; 1994 Oct 12–15; Deauville, France. p. 507–14.
- [6] Miyata T, Yamada H, Hojo T. Aerodynamic response of PE stay cables with pattern-indented surface. In: *Proceedings of the International Conference on Cable-Stayed and Suspension Bridges*; 1994 Oct 12–15; Deauville, France. p. 515–32.
- [7] Yagi T, Okamoto K, Sakaki I, Koroyasu H, Liang Z, Narita S, et al. Modification of surface configurations of stay cables for drag force reduction and aerodynamic stabilization. In: *Proceedings of the 13th International Conference on Wind Engineering*; 2011 July 10–15; Amsterdam, The Netherlands.
- [8] Gu M, Du X. Experimental investigation of rain-wind-induced vibration of cables in cable-stayed bridges and its mitigation. *J Wind Eng Ind Aerod* 2005; 93(1):79–95.